

SPECTRAL POLARIMETRY FOR IDENTIFYING AND SEPARATING MIXED BIOLOGICAL SCATTERERS

Svetlana Bachmann* and Dusan Zrnic

Cooperative Institute for Mesoscale Meteorological Studies, University of Oklahoma
National Severe Storm Laboratory, Norman, Oklahoma

1. INTRODUCTION

Through a good part of spring and fall, strong echoes appear on radar screens starting at sunset and disappearing at sunrise. These have been attributed to migrating birds. We examine one such case of echoes in clear-air planetary boundary layer which occurred during fall of 2004 at the time of nocturnal bird migration. Most of the migratory bird movements occur at altitudes below 3 km with the bulk of action under 900 meters (npwrc.usgs.gov 2005). Bird flight velocity ranges from 8 to 22 m s⁻¹ (Gill 1994).

Many insects also migrate at night. Microinsects are weak flyers, their deliberate or inadvertent motion is primarily wind driven. Insects ascend to altitudes of several hundred meters above the ground where they ride the airstreams crossing many kilometers in a single flight (Chapman et al., 2004). Although their speed can be as high as 8.3 m s⁻¹ (Riley 1999) typical values are 1 m s⁻¹ or less. Thus insects often behave as quasi passive wind tracers. It is this property that makes them suitable for wind measurements with Doppler radars. Thus we submit that lofted insects are excellent scatterers that enhance echoes needed for wind profiling, and that migrating and wandering birds are not passive wind tracers and typically fly at velocities different from those of the wind. We examine Doppler spectra and show that separation of birds from insects is possible if the antenna is pointing in (or near) the direction of the wind. Further spectral densities of dual polarization variables contain discernible signatures that offer a way of distinguishing between birds and insects and obtaining winds aloft.

2. DATA COLLECTION/ RADAR SET UP

Time-series data were collected with the NOAA/NSSL research radar (KOUN) on September 7, 2004 at 11 pm local time (04Z). The radar was in dual polarization mode simultaneously transmitting and receiving waves of horizontal and vertical polarization. The antenna scanned 360° sectors at

elevations 0.5°, 1.5°, 2.5°, 4° and 6° with a pulse repetition time (PRT) of 780 μ s (the unambiguous range R_a and velocity v_a were 117 km and 35 m s⁻¹), as shown in Fig. 1a. The number of samples for spectral analysis was $M = 128$. Spectral moments were obtained and observed in real-time on the plan-position indicator (PPI) displays. Spectral processing and analysis of this data is presented herein.

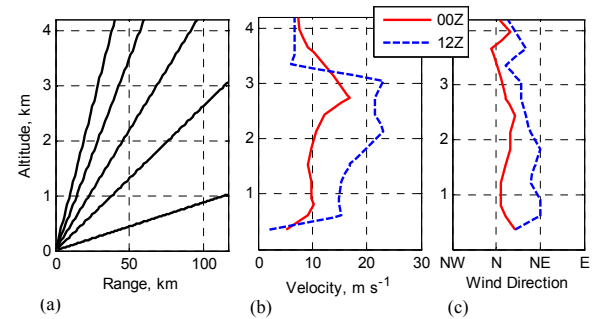


Fig. 1. The altitude information (a) radar elevation scans; (b) wind speed from sounding 2004 September 7/00Z and 7/12Z; (c) wind direction from sounding.

On this day clear-air conditions prevailed over the radar coverage. At time 00Z and 200 m above ground, a North-North-East wind was blowing at 5 m s⁻¹ from 10°; at 800 m it increased to about 10 m s⁻¹ and retained this value throughout the boundary layer (Fig. 1b and 1c). However, the velocities registered on the plan position indicator are much larger, reaching values up to 30 m s⁻¹ (Fig. 3). Radar meteorologists recognize this inconsistency and attribute it to "contamination by biological scatterers"; further they consider such velocities worthless for meteorological interpretation. The purpose of our paper is to demonstrate that spectral analysis and polarimetry can be used to retrieve winds in this and similar situations.

3. DATA ANALYSIS

Significant return power is observed in the horizontal (H) and vertical (V) channels through the boundary layer up to 2.2 km, above which noise dominates. Reflectivity values are relatively low, less than 5 dB. Layers of reflectivity

* Corresponding author address: Svetlana Bachmann, CIMMS, University of Oklahoma, Norman, OK 73019; e-mail: svetlana.bachmann@noaa.gov

corresponding to the altitudes 200 m, 500 m, 800 m, and 1.5 km are evident in elevation scans 1.5°, 2.5°, 4°, and 6° (not shown). The velocities of these layers were larger than background wind velocities. The 800 m layer appears wider and has higher reflectivity values. The 1.5 km layer shows lower reflectivity and the largest velocities. These layered echoes were primarily caused by birds.

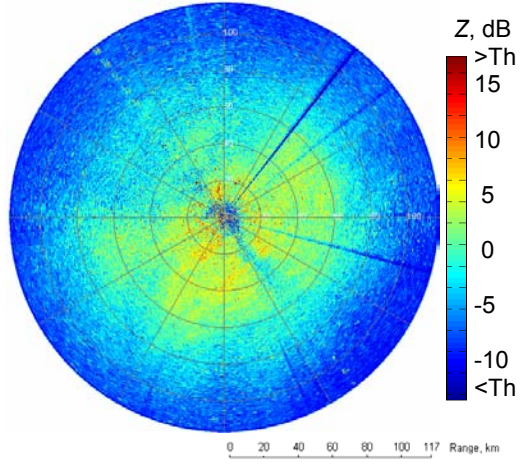


Fig. 2. Reflectivity from H polarization, elevation 0.5°, display ends at $R_a = 117$ km.

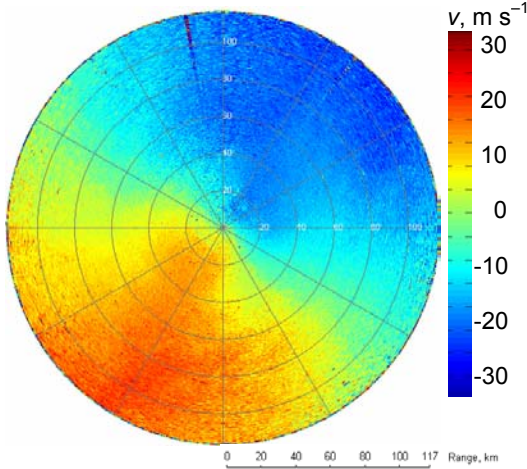


Fig. 3. Velocity from H polarization, elevation 0.5°. The wind direction is NNE. $R_a = 117$ km, and unambiguous velocity, $v_a = 35 \text{ m s}^{-1}$.

4. DISPLAY OF SPECTRA VS RANGE

Fields of Doppler spectral coefficients are presented as a function of radial velocity and range for easier visual interpretation (Fig. 4a); the power of the spectral coefficients (in log base 10 relative units) is color coded. Velocity values are negative for the scatterers moving toward the radar and positive for the ones moving away. One column in the image at

some range R represents the spectrum of the echoes at the range R (Fig. 4b and 4c). In the presence of scatterers the image is expected to display a somewhat continuous color band corresponding to the radial component of the scatterer's velocities. Thus in an ideal case this band represents the dependence of radial velocities on range that should be consistent with the sounding wind profile. Other curves and blobs, which deviate from the band (path) of the main wind, are contaminants. The appearance and explanation are analogues to the case of wind profiling radars whereby often clear-air spectra are contaminated by birds or ground clutter. The contaminants need to be recognized and filtered to avoid errors in the wind estimates.

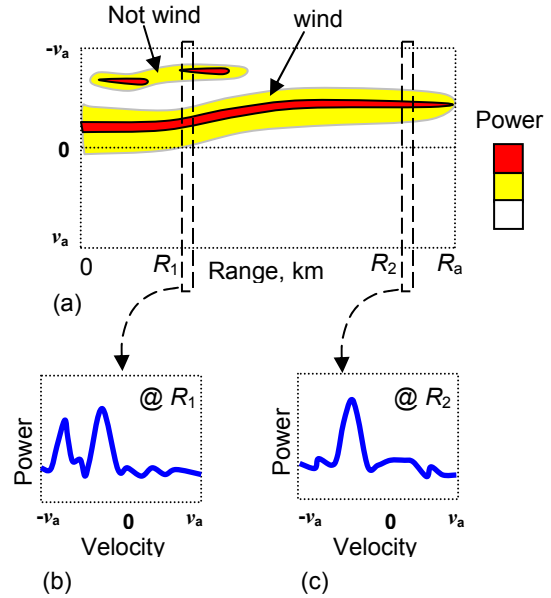


Fig. 4. Explanation of the display of spectra vs range. (a) Field of Doppler spectral coefficients along a radial; colors show power in logarithmic scale, horizontal axis represents range, and the vertical one represents radial velocity from $-v_a$ to v_a ; (b) spectrum at range R_1 ; (c) spectrum at range R_2 . The maxima in spectra are color coded in red.

5. SPECTRAL ANALYSIS

Spectra are weighted with the von Hann window. The preliminary steps for the spectral processing include (1) removing the DC component from all data, (2) filtering the spectral coefficients corresponding to the ground clutter returns where needed, and (3) if desired, applying thresholds to suppress noise. For example, spectra from 30 and 40 km in range at 0.5° elevation, 200° azimuth (Fig. 5a and 5b) demonstrate strong peaks at about 10 m s^{-1} evident in both the H (solid line) and V (dashed line) channels. Additional humps in the spectra at about 20 m s^{-1} differ in the H and V polarizations at 40 km, but the humps at 30 km are similar. The peaks at lower velocities are due to insects and the ones at

higher velocities are from birds. In the spectra from 40 km range the spike at 20 m s^{-1} is bracketed by equally spaced (by 2 m s^{-1}) side peaks. Those are not caused by flapping wings, but rather by birds flying at different speeds. The wing-beat frequency is expected to appear in the spectrum as a pair of side lobe peaks with modulation shift of wing-beat from 0.2 to 0.5 m s^{-1} (5 to 2 Hz). 128 samples do not give enough resolution to observe such small frequency shifts.

The field of Doppler spectral coefficients along the radial at 180° azimuth (Fig. 6) discloses two distinctive bands: one that is continuous (somewhat homogeneous), which stretches along the radial and gradually waves starting at 5 m s^{-1} (near the radar) to 10 (up to 60 km), and to 18 m s^{-1} (beyond 60 km range); and the other which is sporadic and parallels the path of the continuous one but with velocities

larger by about 10 m s^{-1} . The continuous band was observed at all 5 elevations of the scan and in the same as well as adjacent azimuths. The patchy band is mainly present at low elevations; it breaks into segments and blobs at higher elevations. In the presented radial (Fig. 6) separation between the two types of scatterers is very clear. Because of high concentration and lower velocities we deduce that the continuous band is caused by wind blown insects while the patches of the sporadic band are contributions from migrating birds. At azimuths where the bird direction is perpendicular to the radar beam the separation is not apparent due to the overlap of the spectra from birds with those from insects. Investigation of polarimetric properties (next section) further solidifies the assertion that insects and birds shared the airspace throughout most of the boundary layer on that night.

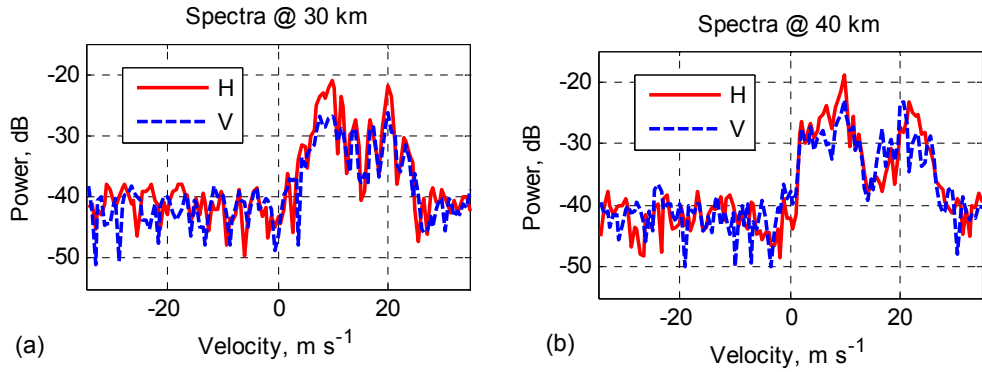


Fig.5. Power spectrum at azimuth 180° , elevation 0.5° , range (a) 30 km; (b) 40 km. The peaks at about 8 m s^{-1} are caused by insects and the peaks at about $20 - 22 \text{ m s}^{-1}$ are caused by birds.

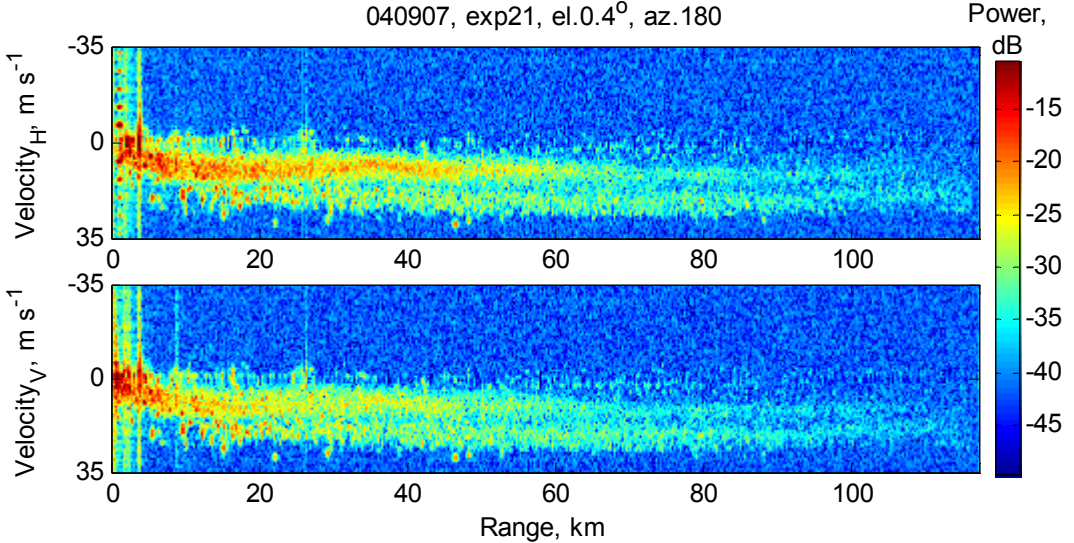


Fig. 6. Fields of Doppler spectral coefficients at azimuth 200° and elevation 0.5° obtained at horizontal (top) and vertical (bottom) polarizations. Negative velocities designate motion toward the radar; positive indicate motion away from the radar. Colors represent power in logarithmic units. The continuous band is due to insects; the blobs of the parallel broken band with faster velocities are caused by migrating birds.

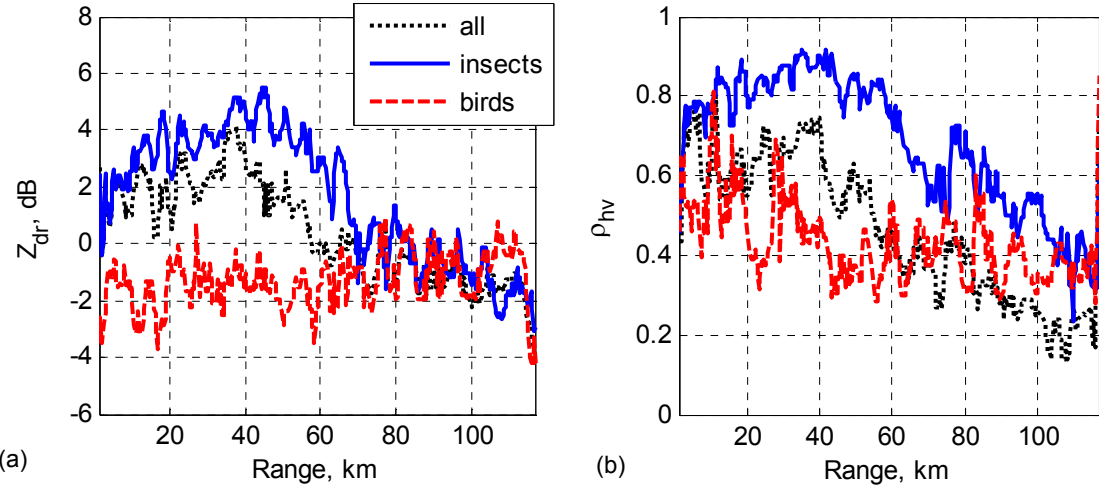


Fig. 7. Z_{dr} and ρ_{hv} computed from SC for radial at azimuth 180° and elevation 0.5° . Beyond 70 km in range the separation is difficult due to noise.

6. SEPARATION USING POLARIMETRIC VARIABLES

Doppler spectra at the two polarizations can be compared and polarimetric variables can be computed from contiguous complex spectral coefficients. The differential reflectivity (Z_{dr}), the copolar correlation coefficient (ρ_{hv}), and the differential phase (ϕ_{dp}) are defined (Zrnić and Ryzhkov 1998) as

$$Z_{dr} = 10 \log_{10} (\langle |s_{hh}|^2 \rangle / \langle |s_{vv}|^2 \rangle),$$

$$|\rho_{hv}(0)| = \langle s_{hh} s_{vv}^* \rangle / [\langle |s_{hh}|^2 \rangle \langle |s_{vv}|^2 \rangle],$$

$$\phi_{dp} = \arg(\rho_{hv}(0)),$$

where s are the scattering coefficients and subscripts denote the transmitted and received polarization.

The polarimetric signatures of insects and birds are substantially different. Insect signatures exhibit high values of Z_{dr} up to 10 dB and moderate values of backscatter ϕ_{dp} of less than 40° . By contrast, bird signatures exhibit lower Z_{dr} from -1 dB to 3 dB but larger values of ϕ_{dp} , sometimes over 100° (Zrnić and Ryzhkov 1998).

The polarimetric variables are computed from complex spectral coefficients at the two polarizations. Spectral coefficients for computing the differential reflectivity (or other polarimetric variables) can be adaptively selected according to signal to noise ratio, or other criteria such as applying a window over a band of velocities. For example, Z_{dr} values computed for a radial at azimuth 180° and elevation 0.5° are shown in Fig. 7a. The dotted curve corresponds to the Z_{dr} computed with the maximum window (i.e., all values of spectral coefficients between -35 and 35 $m s^{-1}$ are included). The solid and dashed lines correspond to the Z_{dr} computed with the window retaining the signal power of presumed

insects (window from 5 to 15 $m s^{-1}$) and birds (window from 16 to 26 $m s^{-1}$), respectively. Likewise windows are used for ρ_{hv} computations (Figure 7b).

Generally, it is hard to distinguish the curves at close ranges due to the ground clutter contamination and at far ranges due to low signal to noise ratio. Nonetheless, separation is clear along most of the radial. In fact, for this azimuth birds and insects have about 5 dB difference in mean differential reflectivity at the ranges 30 to 60 km. The

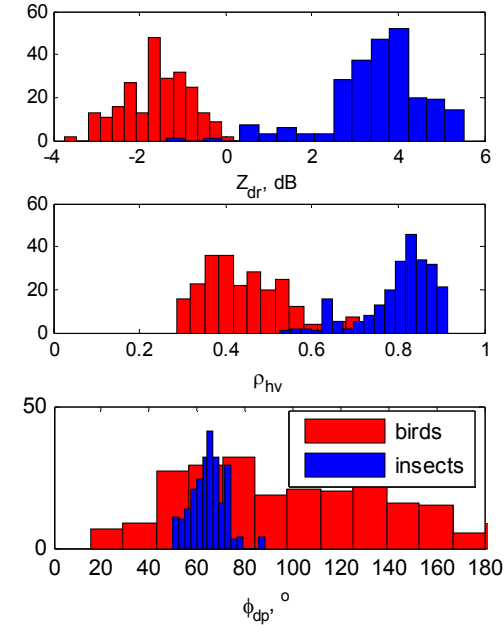


Fig. 8. Histograms of Z_{dr} , ρ_{hv} , and ϕ_{dp} computed from spectral segments designated as insects and birds from the radial at azimuth 180° and elevation 0.5° over ranges from 10 to 70 km.

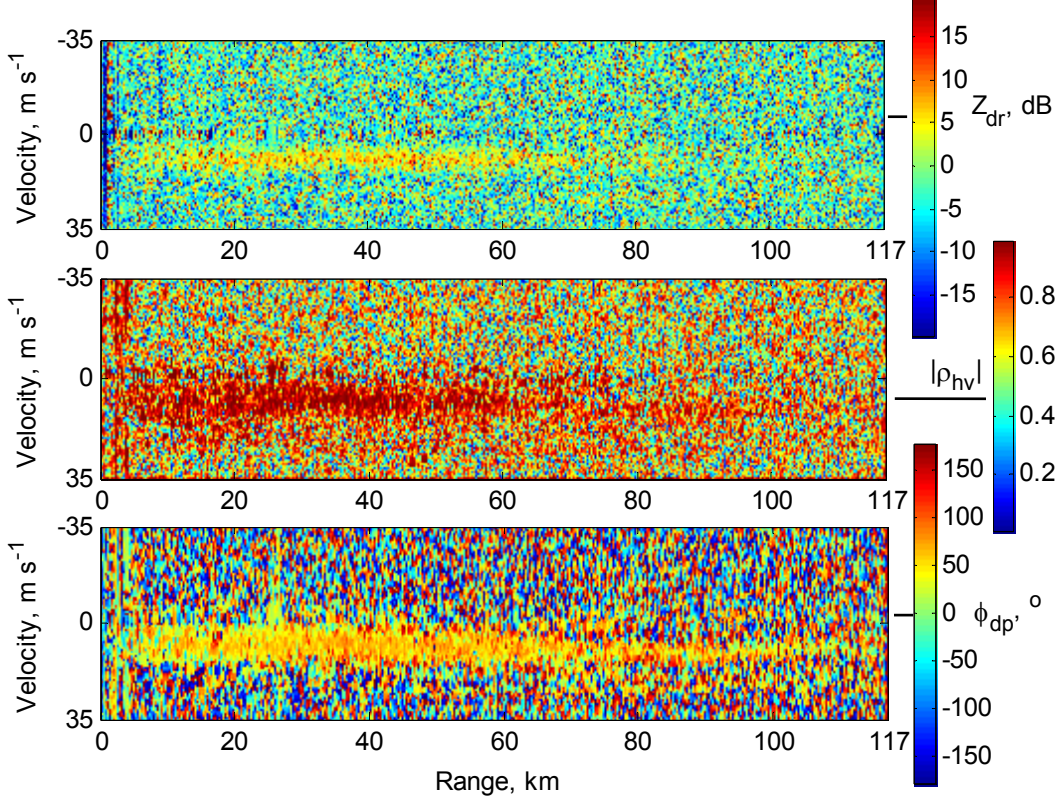


Fig. 9. Spectral densities of polarimetric variables Z_{dr} (top), ρ_{hv} (middle) and ϕ_{dp} (bottom) computed from three point running averages of spectral coefficients.

histograms of Z_{dr} , ρ_{hv} and ϕ_{dp} for the presented radial (Fig. 8), computed for ranges of 10 to 70 km (to diminish the influence of clutter and noise), expose the distinct separation. It is clear that the favorable geometry whereby the beam is pointed in the wind direction tremendously enhances this separation in the spectral densities of the polarimetric variables.

Positioning of the window is not trivial if the wind is changing along a radial, or if its direction is oblique to the beam. The polarimetric variable values depend heavily on the window location and width. To investigate the contribution of the spectral coefficients, we compute the polarimetric variables from three point running averages (of spectral coefficients) along the same radial (Fig. 9). The insects exhibit very well defined Z_{dr} values between 3 dB and 10 dB. The Z_{dr} we attribute to birds is smaller and appears noise like. The copolar correlation coefficient from insects lies in the range 0.7 to 1; it spans much larger values for birds, averaging 0.4 for the presented radial. The differential phase offers a surprisingly good separation with the measurements due to insects appearing as a bright band with values about 68 degrees. The scatterer's phase is computed relative to the system phase; we estimated system phase of the KOUN digital receiver from the ground clutter reflectivity returns (Zrnic et al. 2005). The

differential phase of the insects is found as (phase – system_phase). The differential phase is almost 30° more than the value 40° that was previously reported by Zrnic and Ryzhkov (1998).

The recovered wind velocity is shown in Fig. 10. The streaks can be corrected using velocity azimuth display (VAD) analyses (Fig. 11).

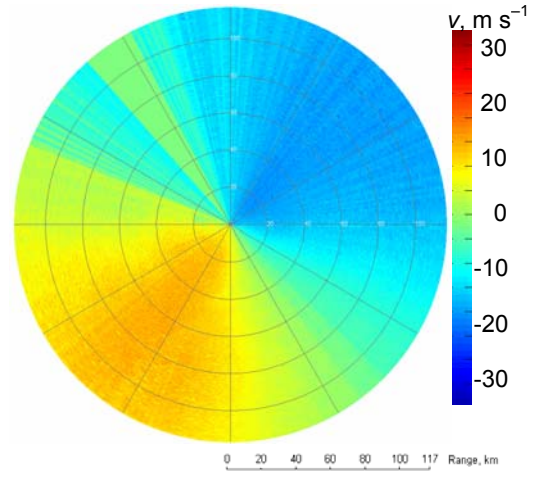


Fig. 10: The recovered field of Doppler wind velocity.

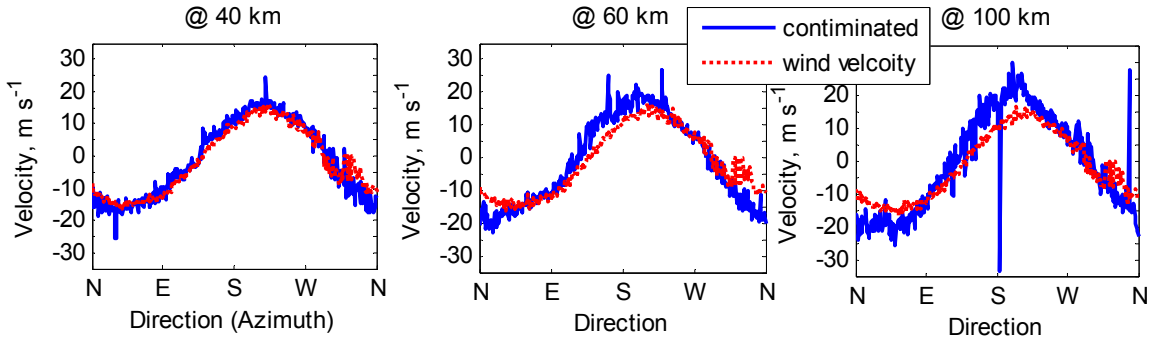


Fig. 11: Velocity azimuth display. Elevation 0.5°.

7. CONCLUSION

Spectral analysis of returns in clear air and at night reveals simultaneous presence of migrating birds and wind blown insects throughout the boundary layer. The separation is facilitated if the antenna beam is pointed in the direction of the wind (coincident with direction of bird flight). Then, the polarimetric variables computed from contiguous sections of the Doppler spectra exhibit almost perfect separation for the two species. The wind data contaminated by migrating birds can be resolved by tracking the wind velocity in range and computing the mean values only from a small set of the spectral coefficients centered on the track (wind band). A decision on the window positioning can be achieved via block analysis of the spectra or by using polarimetric variables. The decision on the window span depends on the total number of samples, on the required accuracy of the estimator and on the position in azimuth. From the spectral densities of the polarimetric variables, it is possible to reconstruct velocity azimuth (VAD) profiles of the wind.

8. REFERENCE

Chapman J. W., D. R. Reynolds, A. D. Smith, E. T. Smith, and I. P. Woiwod, 2004: An aerial netting study of insects migrating at high altitude over England. *Bulletin of Entomological Research*, **94**, 123–136.

Doviak R. J., and D. S. Zrnić, 1984: Doppler Radar and Weather Observations. Academic Press, 458 pp.

Gill F. B., 1994: Ornithology. Freeman & Cia, 766 pp.

Riley, J. R., 1999: Radar returns from insects: Implications for meteorological radars. Preprint 29th Int. Conf. on Radar Meteorology, Montreal, QC, Canada, Amer. Meteor. Soc., 390-393.

Zrnić D. S., and A. V. Ryzhkov, 1998: Observation of Insects and Birds with Polarimetric Radar. *IEEE Trans. Geosci. Remote Sens.*, **36**, 661-668.

Zrnić D. S., V. M. Melnikov, and A.V. Ryzhkov, 2005: Correlation coefficients between horizontally and vertically polarized returns from ground clutter. Submitted to the *Jour. Atmos. Oceanic Technology*